Synthesis, Structure, and Properties of Two New Vanadium(III) Phosphates: $VPO_4 \cdot H_2O$ and $V_{1.23}(PO_4)(OH)_{0.69}(H_2O)_{0.31} \cdot 0.33H_2O$

J. T. Vaughey, William T. A. Harrison, and Allan J. Jacobson*

Department of Chemistry, University of Houston, Houston, Texas 77204

David P. Goshorn and Jack W. Johnson

Exxon Research and Engineering Company, Annandale, New Jersey 08801

Received January 3, 1994®

Two new vanadium(III) phosphates have been synthesized hydrothermally and characterized structurally by Rietveld refinement of X-ray powder diffraction data. The first, $VPO_4 \cdot H_2O$, is monoclinic with a = 6.6953(2) Å, b = 7.7925(3) Å, c = 7.3504(2) Å, and β = 115.255(1)°. The structure was refined in space group $C2/c$ (No. 15). The compound is isostructural with one form of $NiSO_4 \cdot H_2O$ and $MnPO_4 \cdot H_2O$ and closely related to a large class of hydrated divalent metal sulfates with the structure of the mineral kiesserite, $MgSO_4 \cdot H_2O$. The magnetic susceptibility data show Curie–Weiss behavior down to 5 K and are consistent with the presence of all of the vanadium atoms in the trivalent state. The other vanadium(III) phosphate, $V_{1.23}(PO_4)(OH)_{0.69}(H_2O)_{0.31} \cdot 0.33H_2O$, is tetragonal with a = 5.1811(1) Å and c = 12.9329(4) Å. The structure was refined in space group $I4_1/amd$ (No. 141). The compound is isostructural with the mineral caminite, $Mg(SO_4) \cdot xMg(OH)_2 \cdot (1 - 2x)H_2O$, and has magnetic susceptibility behavior indicating strong antiferromagnetic coupling.

Introduction

Since the discovery that $(VO)_2P_2O_7$ is an active and selective catalyst for the mild oxidation of *n*-butane to maleic anhydride, research efforts directed toward the synthesis and characterization of new vanadium phosphate phases have increased dramatically.[1] The number of new phases isolated has been large due to the variety of ways vanadium–oxygen polyhedra (octahedra or square pyramids) and phosphate tetrahedra can be connected to form two- or three-dimensional networks.[2,3] In addition to simple vanadium phosphate phases, the addition of alkali and alkaline earth metals or organic cations, and the development of new synthetic and characterization techniques, has resulted in the isolation of several new phases.[4] In this paper, we report the hydrothermal synthesis and characterization of two new simple vanadium(III) phosphate phases with the stoichiometries $VPO_4 \cdot H_2O$ and $V_{1.23}(PO_4)(OH)_{0.69}(H_2O)_{0.31} \cdot 0.33H_2O$. To date, the only vandium(III) phosphates that have been reported are VPO_4[5] and $V(PO_3)_3$,[6] both of which were synthesized at high temperature.

Experimental Section

Synthesis. $VPO_4 \cdot H_2O$ was synthesized by the reaction of 3.3 mmol of V_2O_5 (Aldrich, 99%). 2.0 mmol of V (powder, Aldrich, 99.9%), 52 mmol of H_3PO_4 (Johnson-Mathey, 85%), and 10 mL of tetraethylammonium hydroxide (TEAOH, Aldrich, 40% in water). The reactants were sealed into a 23-mL Parr bomb and heated to 200 °C for 4 d and then radiatively slow cooled for 2 d to room temperature. The resulting pale green powder was washed with distilled water and allowed to dry under vacuum. The yield based on vanadium was greater than 90%. The same phase was also isolated in the presence of 2 mL of ethylhexylamine or 2 mL of ethylpropylamine in place of TEAOH.

$V_{1.23}(PO_4)(OH)_{0.69}(H_2O)_{0.31} \cdot 0.33H_2O$ was prepared by reaction of 4.4 mmol of V_2O_5 (Aldrich, 99%), 2.6 mmol of V (Aldrich, 99.9%), 52 mmol of H_3PO_4 (Johnson-Mathey, 85%), and 10 mL of tetraethylammonium hydroxide (TEAOH, Aldrich, 40% in water). The reactants were sealed into a 23-mL Parr bomb and heated to 200 °C for 4 d and then radiatively slow cooled for 2 d to room temperature. The dark green powder was washed with distilled water and allowed to dry under vacuum. The yield based on vanadium was greater than 90%. The reaction of V_2O_5 and H_3PO_3 (phosphorous acid, Aldrich, 99%) also yields this phase. The compound has not been prepared using either ethylhexylamine or ethylpropylamine in place of TEAOH.

Structure Determination. The structures of $VPO_4 \cdot H_2O$ and $V_{1.23}(PO_4)(OH)_{0.69}(H_2O)_{0.31} \cdot 0.33H_2O$ were determined by Rietveld refinements against X-ray powder data. High-resolution data were collected for flat plate samples over a 12-h period on a Scintag XDS 2000 powder diffractometer using Cu Kα radiation (λ = 1.5418 Å) operating in a θ–θ geometry between 18 and 100° 2θ with a step size of 0.02° 2θ and a collection time of 8 seconds per point. Patterns were indexed using the program TREOR:[7] $VPO_4 \cdot H_2O$ was indexed on a *C*-centered monoclinic unit cell (figure of merit 26) and $V_{1.23}(PO_4)(OH)_{0.69}(H_2O)_{0.31} \cdot 0.33H_2O$ was indexed on a body-centered tetragonal cell (figure of merit 42). The indexed patterns are shown in Tables 1 and 2. The crystallographic data are given for both phases in Table 3.

The structure of $NiSO_4 \cdot H_2O$ (space group $C2/c$ (No. 15))[8] was taken as the starting model for the $VPO_4 \cdot H_2O$ refinement. Rietveld analysis was carried out using the program GSAS,[9] and the usual profile parameters

® Abstract published in *Advance ACS Abstracts,* April 15, 1994.

(1) (a) Seeboth, H.; Freiberg, H.-J.; Hopf, G.; Kreissig, J.; Kubias, B.; Ladwig, G.; Lucke, B.; Muller, G.; Wolf, H. DDR Patent 113 210, 1975. (b) Seeboth, H.; Kubias, B.; Wolf, H.; Lucke, B. *Chem. Technol.* **1976,** *28,* 730. (c) Wustneck, N.; Wolf, H.; Seeboth, H. *React. Kinet. Catal. Lett.* **1982,** *21,* 497. (d) Bordes, E.; Courtine, P. *J. Chem. Soc. Chem. Commun.* **1985,** 294.

(2) (a) Huan, G.; Johnson, J. W.; Jacobson, A. J.; Corcoran, E. W.; Goshorn, D. P. *J. Solid State Chem.* **1991,** *93,* 514. (b) Amoros, P.; Beltran-Porter, D.; LeBail, G.; Ferey, G.; Villenueve, G. *Eur. J. Solid State Inorg. Chem.* **1991,** *91,* 331. (c) Wang, S. L.; Kang, H. Y.; Cheng, C. Y.; Lii, K. H. *Inorg. Chem.* **1991,** *30,* 3496. (d) Lii, K. H.; Tsai, H. J. *J. Solid State Chem.* **1991,** *91,* 331. (e) Lii, K. H.; Tsai, H. J. *Inorg. Chem.* **1991,** *30,* 446.

(3) (a) Kang, H. Y.; Wang, S. L.; Lii, K. H. *Acta Crystallogr.* **1992,** *C48,* 975. (b) Kang, H. Y.; Lee, W. C.; Wang, S. L.; Lii, K. H. *Inorg. Chem.* **1992,** *31,* 4743.

(4) (a) Soghomonian, V.; Chen Q.; Haushalter, R.; Zubieta, J.; O'Conner, C. *Science* **1993,** *259,* 1596. (b) Soghomonian, V.; Chen, Q.; Haushalter, R.; Zubieta, J. *Angew. Chem., Int. Ed. Engl.* **1993,** *32,* 610.

(5) (a) Ladwig, G.; Jost, K. H.; Schlesinger, K. *Z. Chem.* **1979,** *19,* 386. (b) Tudo, J.; Carton, D. *C. R. Acad. Sci., Ser. C (Paris)* **1979,** *289,* 219.

(6) Tofield, B.; Crane, G. R.; Pastuer, G.; Sherwood, R. *J. Chem. Soc., Dalton Trans.* **1975,** 1806.

(7) Werner, P. E. *Z. Kristallogr.* **1969,** *120,* 375.

(8) Le Fur, Y.; Coing-Boyat, J.; Bassi, G. *C. R. Acad. Sci., Ser. C (Paris)* **1966,** *262,* 632.

(9) Von Dreele, R. B.; Larson, A. C. *GSAS Users Guide*; Los Alamos National Laboratory: Los Alamos, NM, 1985–1992.

0020-1669/94/1333-2481$04.50/0

Table 1. Observed and Calculated *d*-Spacings (Å) for $VPO_4 \cdot H_2O$[a]

hkl	d_{obs}	d_{calc}[b]	I_{obs}	I_{calc}[c]
110	4.784	4.782	50	50
11$\bar{1}$	4.707	4.707	63	56
020	3.899	3.901	7	8
111	3.380	3.383	100	100
11$\bar{2}$	3.300	3.303	25	27
20$\bar{2}$	2.953	2.954	38	29
022	2.531	2.522	48	51
220	2.391	2.393	1	1
13$\bar{1}$	2.379	2.380	14	13
31$\bar{1}$	2.129	2.129	15	16
13$\bar{2}$	2.116	2.117	10	10
221	2.042	2.043	16	16
040	1.949	1.948	3	3
023	1.927	1.928	2	2
31$\bar{3}$	1.908	1.909	12	13
202	1.876	1.877	5	6
113	1.794	1.795	6	9
222	1.690	1.691	3	3
24$\bar{1}$	1.684	1.683	3	2
042	1.681	1.682	7	8
22$\bar{4}$	1.650	1.652	12	16
240	1.639	1.640	13	13
330	1.595	1.596	1	1
33$\bar{3}$	1.569	1.570	9	10
42$\bar{2}$	1.538	1.539	5	6
400	1.514	1.515	6	10
133	1.504	1.504	6	10
331	1.444	1.445	3	3
151	1.440	1.441	4	5
31$\bar{5}$	1.401	1.402	3	4
24$\bar{4}$	1.331	1.331	2	2
15$\bar{3}$	1.315	1.316	2	2
51$\bar{1}$	1.274	1.276	5	2
44$\bar{2}$	1.270	1.271	6	5
20$\bar{6}$	1.222	1.223	2	4
26$\bar{2}$	1.189	1.190	4	4

[a] Unit cell: a = 6.6968(6) Å, b = 7.7971(4) Å, c = 7.3526(7) Å, β = 115.257(7)°, V = 347.22(6) Å^3. Space group: $C2/c$ (No. 15). [b] Calculated *d*-spacings are based on least-squares refinement using the program TREOR.[7] [c] Intensities were calculated using the program LAZY-PULVERIX.[24]

(scale factor, background polynomial coefficients, zero-point error, pseudo-Voigt peak shape width variation descriptors), and atomic positional and thermal parameters were added to the model as variables in the usual fashion. This model successfully converged to final residuals of R_p = 8.83% and R_{wp} = 11.62% for 26 parameters and 2114 data points. The final Rietveld observed, calculated, and difference plots are shown in Figure 1. Final atomic positional and thermal parameters are presented in Table 4, and selected bond distance/angle data for $VPO_4 \cdot H_2O$ are given in Table 5.

The structure of $V_{1.23}(PO_4)(OH)_{0.69}(H_2O)_{0.31} \cdot 0.33H_2O$ was optimized in a similar fashion, with the structure of $MgSO_4 \cdot 1/3Mg(OH)_2 \cdot 1/3H_2O$ (space group $I4_1/amd$ (No. 141)) taken as the starting model.[10,11] After refinement of the usual profile, atomic positional and thermal parameters, and the vanadium site occupancy (*vide infra*), final residuals of R_p = 7.75% and R_{wp} = 9.49% for 21 parameters and 2099 data points were obtained. The final Rietveld observed, calculated, and difference plots are shown in Figure 2. Final atomic positional and thermal parameters are presented in Table 6, and selected bond distance/angle data for $V_{1.23}(PO_4)(OH)_{0.69}(H_2O)_{0.31} \cdot 0.33H_2O$ are given in Table 7. The final stoichiometry derived from the X-ray refinement was $V_{1.23}(PO_4)O$. At the end of the refinement, no reasonable proton positions were apparent in Fourier difference maps. Assuming that all of the vanadium atoms are present as V^{3+}, the stoichiometry can be written as $V_{1.23}(PO_4)(OH)_{0.69}(H_2O)_{0.31}$, but further characterization (see below) indicated the presence of additional water molecules.

Characterization

Thermogravimetric analysis of each compound was carried out to determine the water content using a TA Instruments Hi-Res 2950 thermogravimetric analyzer: Each compound was heated at 5 °C/min up to 600 °C in dry nitrogen. $VPO_4 \cdot H_2O$ lost 9.89(1)% of its weight in three steps, at 393, 420, and 543 °C, corresponding to (if all due to water loss) a stoichiometry of $VPO_4 \cdot 0.9H_2O$. A slight variation in water content is commonly observed in these types of systems,[3] so the formula will hereafter be written as $VPO_4 \cdot H_2O$.

The compound $V_{1.23}(PO_4)(OH)_{0.69}(H_2O)_{0.31} \cdot nH_2O$ lost 9.4(2)% of its weight under similar conditions, except that the final temperature had to be raised to 750 °C to complete the decomposition. The weight loss occurred in three steps: 267, 442, and 522 °C. The total weight loss corresponds to a stoichiometry of $V_{1.23}(PO_4)(OH)_{0.69}(H_2O)_{0.31} \cdot 0.29(2)H_2O$, assuming the final products are VPO_4 and V_2O_3. In order to confirm the presence of additional water molecules, thermogravimetric analysis was also carried out under the same conditions but in oxygen rather than nitrogen. In oxygen, the weight first decreased due to dehydration and then increased on oxidation of V^{3+} to V^{5+}. The final products were identified by X-ray diffraction as

Table 2. Observed and Calculated *d*-Spacings (Å) for $V_{1.23}(PO_4)(OH)_{0.69}(H_2O)_{0.31} \cdot 0.33H_2O$

hkl	d_{obs}	d_{calc}[b]	I_{obs}	I_{calc}[c]
101	4.809	4.813	3	3
103	3.313	3.313	100	100
112	3.187	3.190	52	46
200	2.592	2.593	14	11
211	2.281	2.283	12	13
213	2.041	2.041	24	20
204	2.021	2.023	9	9
116	1.858	1.859	5	6
220	1.832	1.834	9	8
206	1.657	1.657	17	18
303	1.603	1.604	10	9
224	1.594	1.595	23	22
312	1.589	1.589	8	6
217	1.446	1.445	6	8
305	1.438	1.436	1	1
321	1.429	1.427	2	2
208	1.373	1.372	1	2
323	1.364	1.363	2	3
316	1.305	1.304	3	4
400	1.296	1.295	8	9
219	1.222	1.222	2	3
413	1.207	1.206	3	5
332	1.200	1.200	1	1
2,0,10	1.158	1.157	3	5
327	1.135	1.134	2	3

[a] Unit cell: a = 5.1819(4) Å, c = 12.927(2) Å, V = 347.13(4) Å^3. Space group: $I4_1/amd$ (No. 141). [b] Calculated *d*-spacings are based on least-squares refinement using the program TREOR.[7] [c] Intensities were calculated using the program LAZY-PULVERIX.[24]

Table 3. Crystallographic Parameters

	$VPO_4 \cdot H_2O$	$V_{1.23}PO_4(OH)_{0.69}(H_2O)_{0.31} \cdot 0.33H_2O$
emp formula	$V_1P_1O_5H_2$	$V_{1.23}P_1O_{5.33}H_{1.97}$
mol wt	163.93	180.89
crystal system	monoclinic	tetragonal
a (Å)	6.6954(3)	5.1811(2)
b (Å)	7.7925(3)	5.1811(2)
c (Å)	7.3504(3)	12.9329(4)
β (deg)	115.255(1)	90
V (Å^3)	346.84(3)	347.17(3)
Z	4	4
space group	$C2/c$ (No. 15)	$I4_1/amd$ (No. 141)
T (°C)	25(2)	25(2)
λ(Cu Kα) (Å)	1.54178	1.54178
ρ_{calc} (g/cm^3)	3.139	3.461
no. of data points	2114	2099
R_p[a] (%)	8.83	7.50
R_{wp}[b] (%)	11.62	9.49

[a] $R_p = \Sigma|y_o - Cy_c|/\Sigma|y_o|$. [b] $R_{wp} = [\Sigma w(y_o - C\,y_c)^2/\Sigma w y_o^2]^{1/2}$, where C is a scale factor.

(10) Yamnova, N. A.; Pushcharovskii, D. Y.; Apollonov, V. N. *Vestn. Mosk. Univ., Geol.* **1989**, *5*, 73.
(11) Keefer, K. D.; Hochella, M. F., Jr.; De Jong, B. H. W. S. *Acta Crystallogr.* **1981**, *B37*, 1003.

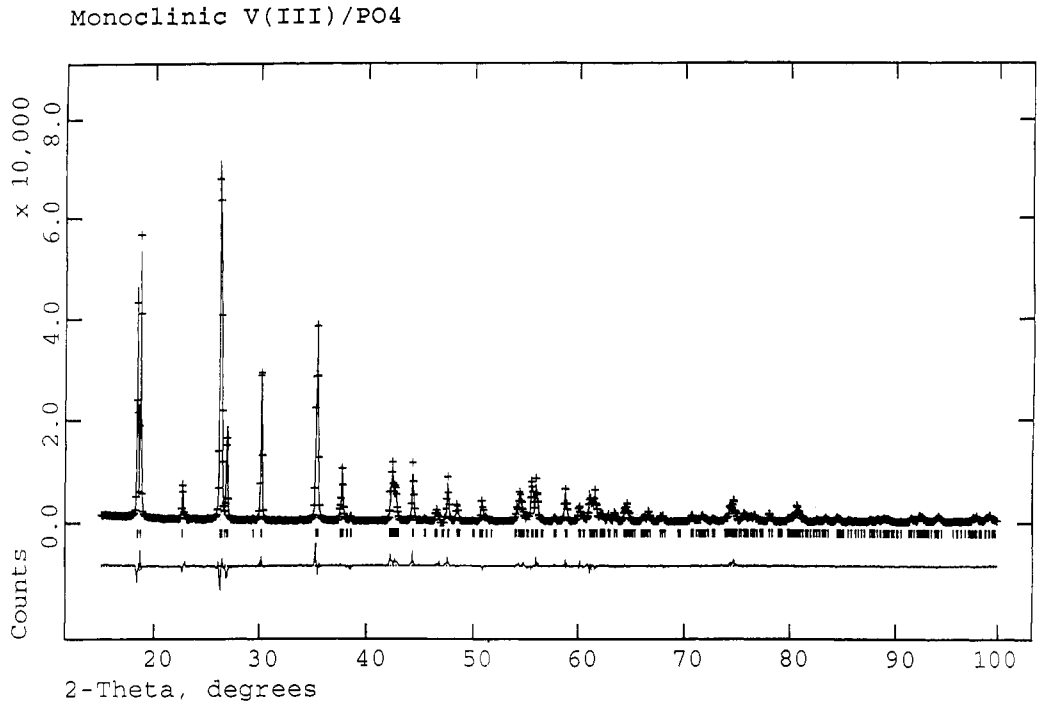

Figure 1. Observed and calculated X-ray powder pattern for $VPO_4 \cdot H_2O$. The pluses are the data points, and the solid line is the fit to the data using the reported model. The small lines below indicate the predicted peak locations.

Table 4. Final Atomic, Positional, and Thermal Parameters for $VPO_4 \cdot H_2O$

atom	x	y	z	U_{iso} (Å²)	occ
V	0.25	0.25	0	0.0016(5)	1.0
P	0	0.0829(4)	0.25	0.0016(5)	1.0
O1	0.2131(8)	−0.0306(6)	0.3549(7)	0.01	1.0
O2	0.0230(7)	0.1946(5)	0.0889(7)	0.01	1.0
O3[a]	0	0.6162(8)	0.25	0.01	1.0

[a] Oxygen atom O3 is the oxygen atom of the water molecule.

Table 5. Selected Bond Distances (Å) and Angles (deg) $VPO_4 \cdot H_2O$

		Distances			
V–O1	1.974(5)	×2	P–O1	1.573(5)	×2
V–O2	1.942(4)	×2	P–O2	1.530(5)	×2
V–O3	2.154(3)	×2			
		Angles			
O1–V–O1	180		O2–V–O3	87.7(1)	×2
O1–V–O2	86.9(2)	×2		92.3(1)	×2
	93.1(2)	×2	O3–V–O3	180	
O1–V–O3	94.9(2)	×2	O1–V–O1	111.6(4)	
	85.1(9)	×2	O1–P–O2	109.2(2)	×2
O2–V–O2	180			108.1(3)	×2
			O2–P–O2	110.6(4)	

Table 6. Final Atomic, Positional, and Thermal Parameters for $V_{1.23}(PO_4)(OH)_{0.69}(H_2O)_{0.31} \cdot 0.33H_2O$

atom	x	y	z	U_{iso} (Å)²	occ
V	0	0	0.5	0.0096(8)	0.615(4)
P	0	0.75	0.125	0.0082(8)	1.0
O1	0	0.5075(5)	0.1921(2)	0.0082(9)	1.0
O2[a]	0	0.25	0.375	0.0082(9)	1.0

[a] Oxygen atom O2 is from the OH/H_2O.

β-$VOPO_4$ and V_2O_5. The overall weight gain was 0.007(1)%, corresponding to n = 0.37(1) in the above formula. The thermogravimetric experiments were repeated several times to ensure reproducibility. An average value of 0.33(4) will be used for the final formula.

Elemental analysis of $V_{1.23}(PO_4)(OH)_{0.69}(H_2O)_{0.31} \cdot 0.33H_2O$ was carried out by Galbraith Laboratories of Knoxville, TN. The elemental analysis gave 34.7% V and 17.1% P, corresponding to a V/P ratio of 1.23:1 in good agreement with the ratio determined from the X-ray structure refinement. The calculated weight percentages based on the composition determined using the thermogravimetric analysis data were 34.6% V and 17.1% P, in excellent agreement with the overall formulation $V_{1.23}(PO_4)(OH)_{0.69}(H_2O)_{0.31} \cdot 0.33H_2O$.

Table 7. Selected Bond Distances (Å) and Angles (deg) for $V_{1.23}(PO_4)(OH)_{0.69}(H_2O)_{0.31} \cdot 0.33H_2O$

		Distances			
V–O1	2.004(2)	×4	V–V	2.5905(5)	
V–O2	2.0715(4)	×2	P–O1	1.527(3)	×4
		Angles			
O1–V–O1	180	×2	O1–V–O3	94.9(2)	×2
	83.4(1)	×2		85.1(9)	×2
	96.6(1)	×2	O2–V–O2	180	
O1–V–O2	83.5(1)	×4	O1–P–O1	108.84(9)	×4
	96.5(1)	×4		110.7(2)	×2

Magnetic susceptibility data were obtained from 4.2 to 300 K in an applied field of 6 kG using a Quantum Design Model MPMS SQUID Magnetometer. Ferromagnetic impurity contributions to the magnetic susceptibility were measured and corrected for via magnetization isotherms obtained at 77 and 298 K. The susceptibility data for the compound $VPO_4 \cdot H_2O$ were modeled over the complete temperature range according to the Curie–Weiss law, $\chi = \chi_0 + C/(T - \Theta)$. In the final fit, $\chi_0 = -6.9532 \times 10^{-7}$ emu/g, $C = 5.549 \times 10^{-3}$ emu/g·K, and $\Theta = 1.0$ K. The high-temperature data for $V_{1.23}(PO_4)(OH)_{0.69}(H_2O)_{0.31} \cdot 0.33H_2O$ were also modeled using the Curie–Weiss law in the approximately linear region from 100 to 300 K. The values were found to be $\chi_0 = -2.1271 \times 10^{-6}$ emu/g, $C = 9.4872 \times 10^{-3}$ emu/g·K, and $\Theta = -238$ K.

Results

Monoclinic $VPO_4 \cdot H_2O$ is isostructural with one form of $NiSO_4 \cdot H_2O$[10] and $MnPO_4 \cdot H_2O$.[12] The structure is built up from vertex-sharing chains of VO_6 octahedra connected along the [101] direction. Each chain is connected by phosphate groups that bridge two vanadium octahedra in one chain to two other chains. The oxygen atom of the water molecule, O(3), connects the

(12) Lightfoot, P.; Cheetham, A. K.; Sleight, A. W. *Inorg. Chem.* **1987**, *26*, 3544.

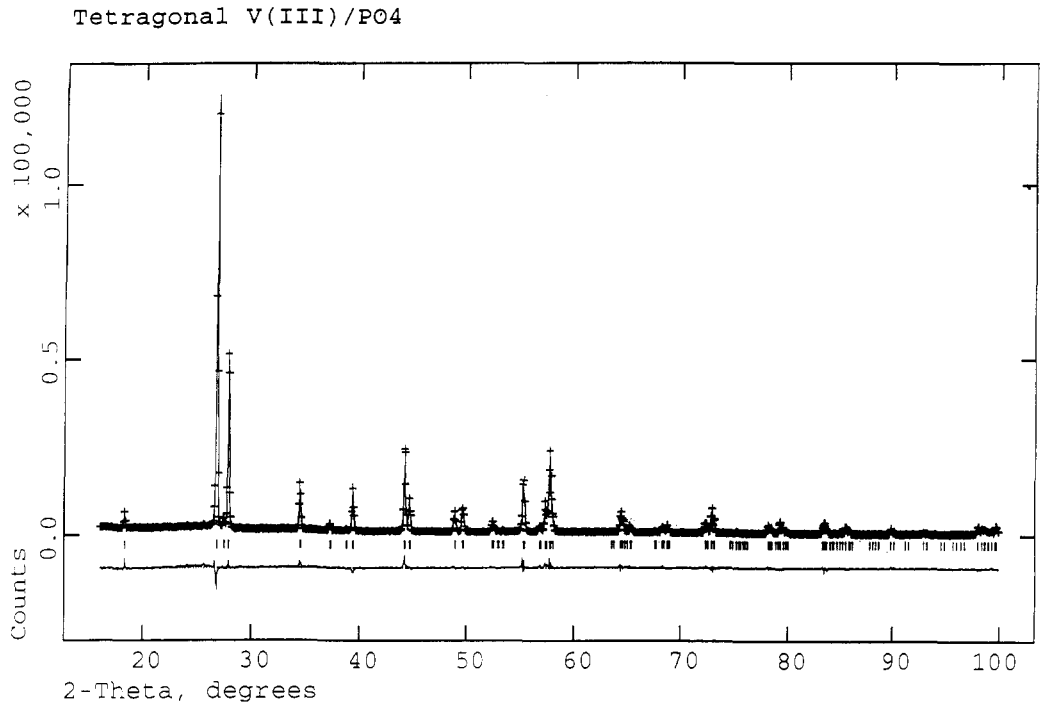

Figure 2. Observed and calculated X-ray powder pattern for $V_{1.23}(PO_4)(OH)_{0.69}(H_2O)_{0.31}\cdot 0.33H_2O$. The pluses are the data points, and the solid line is the fit to the data using the reported model. The small lines below indicate the predicted peak locations.

vanadium cations in the [V–O–V] chain. The vanadium cations are octahedrally coordinated with an average bond distance characteristic of vanadium(III) (d_{avg} = 2.023(2) Å). There are no "unusually" short metal oxygen distances or octahedral distortions that would indicate vanadium(IV) or vanadium(V) cations. The structure is shown in Figure 3.

$V_{1.23}(PO_4)(OH)_{0.69}(H_2O)_{0.31}\cdot 0.33H_2O$ is tetragonal and isostructural with the mineral caminite $Mg(SO_4)\cdot xMg(OH)_2\cdot(1-2x)H_2O$.[11] In contrast to the monoclinic vanadium phosphate phase, $VPO_4\cdot H_2O$, the tetragonal phase is composed of chains of face-sharing vanadium/oxygen octahedra connected in the *ab* plane by two oxygen atoms of the phosphate groups. The other two oxygen atoms of the phosphate groups connect to orthogonal chains of face-sharing vanadium/oxygen octahedra. Four octahedra share a common oxygen atom at the intersection of the orthogonal chains. The structure is shown in Figure 4. At the ideal composition $V_{1.33}$, the vanadium cations would occupy $^2/_3$ of the sites in the face-sharing octahedral chain and an ordered arrangement in which each pair of vanadium cations share only one octahedron face is possible. No evidence of supercell lines to indicate a long-range ordering of the vanadium cations was observed in the powder diffraction data. The X-ray data do not distinguish between a random distribution of vanadium atom vacancies over all chain sites and the situation in which vacancies are ordered in individual chains with no correlation between chains. The elemental and thermogravimetric analysis data indicate the presence of an additional 0.33 molecules of water that are not detected by X-ray diffraction and are presumably disordered.

A related compound, $Fe_{1.21}PO_4X$ (X = OH, F, H_2O), was recently reported by Loiseau et al., and a similar overall structure and stoichiometry were observed in their single-crystal studies.[13]

When heated in a nitrogen atmosphere at 700 °C, both compounds dehydrate and form a brown phase. The powder X-ray diffraction data for the products of the reaction resembled the results for the tetragonal phase. Several extra reflections were observed, however, that could only be indexed with an orthorhombic cell. The X-ray data for the brown anhydrous phase were indexed using the program TREOR,[7] and cell constants

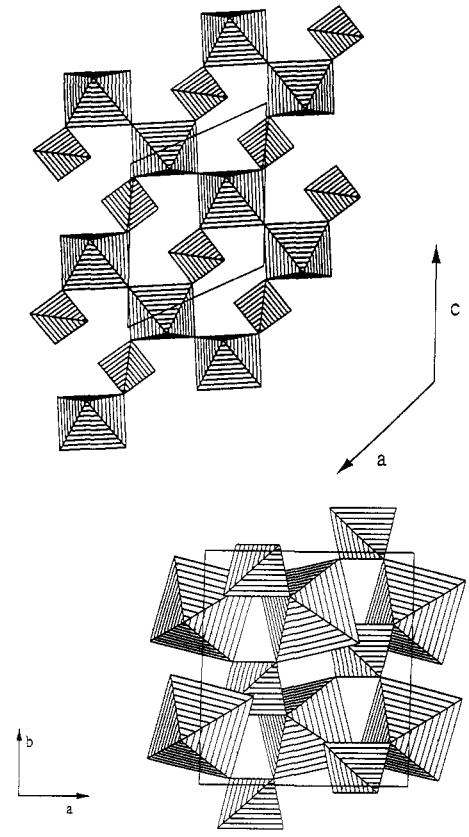

Figure 3. (a, Top) Structure of $VPO_4\cdot H_2O$ showing the vanadium/oxygen octahedra corner-sharing chains and their connectivity via the phosphate groups. The view is in the [010] direction. (b, Bottom) Vanadium–oxygen octahedra/phosphate tetrahedra representation of the $VPO_4\cdot H_2O$ structure showing how phosphates bridge the vanadium octahedral chains in the *b*-direction, viewed down the [100] direction.

a = 7.327(2) Å, b = 7.246(2) Å, and c = 12.844(4) Å (figure of merit for 16 peaks = 9) were obtained. The orthorhombic cell is related to the tetragonal cell of $V_{1.23}(PO_4)(OH)_{0.69}(H_2O)_{0.31}\cdot 0.33H_2O$ by the relationship $a_O \approx \sqrt{2}a_T$, $b_O \approx \sqrt{2}a_T$, and $c_O \approx c_T$. The dehydration process that produces the brown phase

(13) Loiseau, T.; LaCorre, P.; Calage, Y.; Greneche, J. M.; Ferey, G. *J. Solid State Chem.* **1993**, *105*, 417.

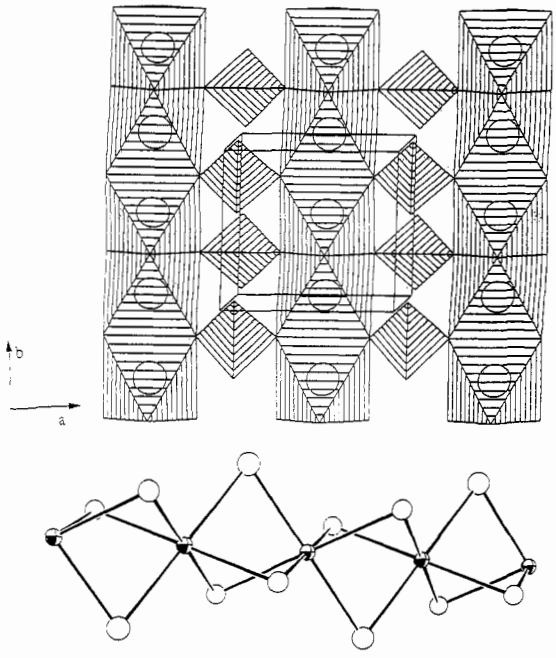

Figure 4. (a, Top) Structure of $V_{1.23}(PO_4)(OH)_{0.69}(H_2O)_{0.31}\cdot 0.33H_2O$ showing the face-sharing vandium–oxygen octahedral chains and the tetrahedral phosphate groups, viewed down the [001] direction. The circles represent the positions of the vanadium sites. (b, Bottom) An isolated segment from the vanadium/oxygen octahedra face-sharing chain.

introduces significant line broadening in the X-ray data, and consequently no attempt was made to determine the detailed structure.

Further heating to 1000 °C in a nitrogen atmosphere produced the high-temperature form of VPO_4 (with the β-$CrPO_4$ structure).[5] Upon being heated in air or oxygen, both compounds dehydrate and oxidize in one step around 500 °C to form β-$VOPO_4$.[14] In addition, after dehydration of $V_{1.23}(PO_4)(OH)_{0.69}(H_2O)_{0.31}\cdot 0.33H_2O$ under oxygen, V_2O_5 was identified as a product by powder X-ray diffraction, accounting for the extra vanadium in the starting material relative to that in the final decomposition product.

Magnetic measurements for $VPO_4\cdot H_2O$ show an observed moment of 2.85 μ_B, in good agreement with that normally observed for vanadium(III) compounds and no indication of any long-range magnetic interactions. For $V_{1.23}(PO_4)(OH)_{0.69}(H_2O)_{0.31}\cdot 0.33H_2O$, the apparent moment determined from the nearly linear region above 100 K is 3.35 μ_B/vanadium, outside of the range predicted for vanadium(III) compounds. Below 100 K, however, complex magnetic behavior is observed due to antiferromagnetic exchange coupling between vanadium atoms present in chains of different length. The exchange coupling influences the apparent moment calculated with the assumption of Curie–Weiss behavior in the temperature range 200–300 K (see below). The data are shown in Figures 5 and 6.

Discussion

Vanadium phosphate compounds have received a wide amount of interest due to their catalytic properties and the wide variety of structures observed. The two new compounds described in this paper have similar compositions but very different structures. The only apparent difference in synthetic conditions is the concentration of vanadium in solution, with slightly higher concentrations favoring the tetragonal phase. The pH is similar in the two preparations and is largely determined by the large excess of amine present. Different syntheses showed no evidence for any significant variation in the V/P ratio in $V_{1.23}(PO_4)(OH)_{0.69}(H_2O)_{0.31}\cdot 0.33H_2O$.

(14) Bordes, E.; Courtine, P.; Pannetier, G. *Ann. Chem.* **1973**, *8*(2), 105.

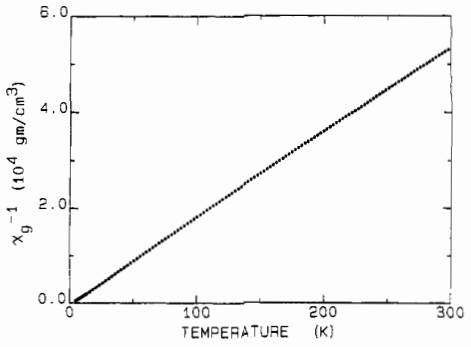

Figure 5. Inverse gram susceptibility data versus temperature for $VPO_4\cdot H_2O$.

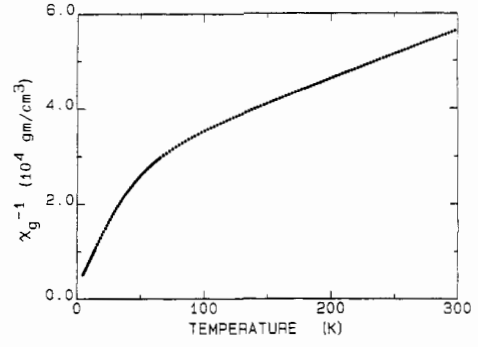

Figure 6. Inverse gram susceptibility data versus temperature for $V_{1.23}(PO_4)(OH)_{0.69}(H_2O)_{0.31}\cdot 0.33H_2O$.

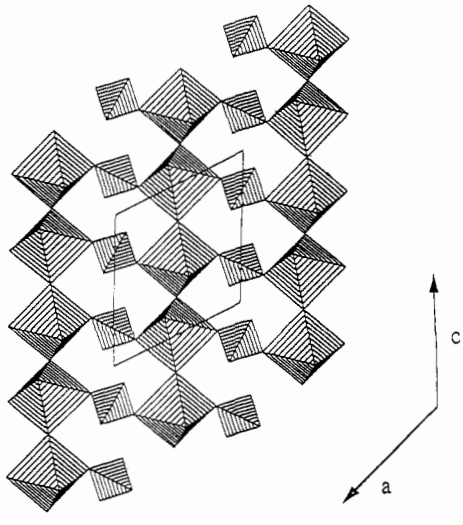

Figure 7. Magnesium–oxygen octahedral chains in $MgSO_4\cdot H_2O$ (kieserite) viewed down the [010] direction (compare to Figure 3a).

The monoclinic $VPO_4\cdot H_2O$ phase is isostructural with $MnPO_4\cdot H_2O$ and $NiSO_4\cdot H_2O$. Although there are many divalent metal sulfates with this same stoichiometry, $MSO_4\cdot H_2O$ (M = Ni, Mg, Zn, Mn, Co, Fe), most have the structure of the mineral kieserite, $MgSO_4\cdot H_2O$,[15] which is closely related to the $VPO_4\cdot H_2O$ structure, except for the orientation of the corner-sharing MO_6 octahedral chains. In the kieserite structure, the chains run along the [001] direction, while in the $VPO_4\cdot H_2O$ structure they run along the [101] direction. For comparison, the octahedral chain in $MgSO_4\cdot H_2O$ (kieserite) is shown in Figure 7 in the same orientation as Figure 3. The $VPO_4\cdot H_2O$ structure is also closely related to the β-$VOPO_4$ structure, in which the oxygen of the water molecule in $VPO_4\cdot H_2O$ assumes the structural role of the short [V–O] bond in β-$VOPO_4$. The relationship is shown in

(15) (a) Bregeault, J.-M.; Herpin, P.; Manoli, J.-M.; Pannetier, G. *Bull. Soc. Chim. Fr.* **1970**, 4243. (b) Bregeault, J.-M.; Herpin, P.; Coing-Boyat *Bull. Soc. Chim. Fr.* **1972**, 2247.

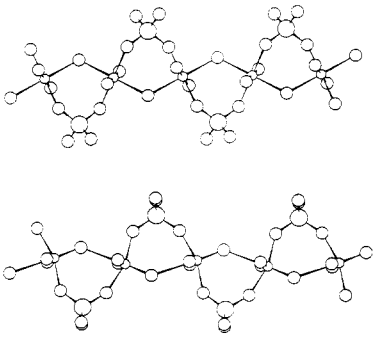

Figure 8. Comparison of the V–O–V chain from $VPO_4 \cdot H_2O$ (top) and β-$VOPO_4$ (bottom).

Figure 8. The main difference between the two chains is the orientation of the phosphate group connecting the two vanadium octahedra. In $VPO_4 \cdot H_2O$, the phosphate group is more canted than in β-$VOPO_4$. This slight difference is probably a result of the closer distance between vanadium centers (3.77 Å vs 3.89 Å) and the more acute V–O–V bond angle (122.11° vs 137.71°) that may result from the difference in formal oxidation state and preferred coordination. This close relationship may explain the rapid conversion of $VPO_4 \cdot H_2O$ to β-$VOPO_4$ upon heating in air. In addition, it was found that heating β-$VOPO_4$ impregnated with 2 wt % platinum (as H_2PtCl_6) under hydrogen at 150 °C for 2 d resulted in the reconversion back to $VPO_4 \cdot H_2O$. No reaction was observed to occur in the absence of platinum up to 250 °C.

The tetragonal $V_{1.23}(PO_4)(OH)_{0.69}(H_2O)_{0.31} \cdot 0.33H_2O$ phase is isostructural with caminite, $Mg(SO_4) \cdot xMg(OH)_2 \cdot (1 - 2x)H_2O$.[11,16,17] The structure of $V_{1.23}(PO_4)(OH)_{0.69}(H_2O)_{0.31} \cdot 0.33H_2O$ is constructed from columns of face-sharing vanadium(III) octahedra, connected by phosphate groups. Face-sharing octahedra are relatively uncommon in vanadium phosphate chemistry, although they are observed in $VO(HPO_4) \cdot 0.5H_2O$.[18,19] The chains in $V_{1.23}(PO_4)(OH)_{0.69}(H_2O)_{0.31} \cdot 0.33H_2O$ are only partially occupied (61.5%) by vanadium atoms. The vanadium occupancy is lower than expecdted for the ideal stoichiometry of $V_4(PO_4)(OH)_3$. To our knowledge, no V(III) compound with this ideal stoichiometry has been reported, but a phase prepared at high pressure with the composition $V_4(PO_4)O(OH)_2$ is closely related.[20] The unit cell of this compound, containing three V^{3+} cations and one V^{4+} cation, is closely similar to that of $Fe_4(PO_4)(OH)_3$. The structure of the latter was determined by single-crystal X-ray diffraction and contains chains of face-sharing oxygen octahedra that are occupied in an ordered way by Fe^{3+} cations and vacancies, resulting in the formation of Fe_2O_9 dimers. The chains in the ordered monoclinic structures are closely similar to those in the disordered tetragonal phase reported here and in the $Fe_{1.21}PO_4X$ structure.[13]

For a random distribution of vanadium atoms within a chain, the average length of a vanadium atom chain V_n corresponds to $n = 2.57$. In a random distribution, a substantial fraction of the vanadium atoms are present as dimers but there is also a significant population of longer chain units. The presence of vanadium atoms in face-sharing chains is expected to become increasingly unfavorable as the value of n increases because of electrostatic repulsions between V^{3+} cations across the octahedral faces. In shorter chains, the unfavorable electrostatic interactions can be reduced by local vanadium atom displacements. Consequently, the distribution is expected to favor the formation of dimers rather than being purely random. A V/P = 1.33 composition permits a regular arrangement of dimers and vacancies along each chain, as found in $Fe_4(PO_4)(OH)_3$. The lower observed V/P ratio suggests that even dimer formation is unfavorable though it may also reflect the energy consequence of different possible occupancies of the four octahedra present at chain intersections. A similar value is found for the chain occupancy in the structurally analogous iron compounds, $Fe_{1.21}(PO_4)X$.[13] The behavior of the magnetic susceptibility data with temperature can be accounted for by antiferromagnetic exchange coupling between the vanadium atoms present as dimers[21] (or in longer chains), together with a contribution from isolated V^{3+} ions. The general shape of the data is reproduced by a Curie term for the isolated V^{3+} ions combined with an exchange coupled dimer susceptibility of the form[21]

$$\chi_M = \mu_{eff}^2 N \mu_B^2 (e^{2J/kT} + 5e^{6J/kT})/(1 + 3e^{2J/kT} + 5e^{6J/kT})kT$$

with $J/k = -100$ K. This model predicts, using a typical μ_{eff} for V^{3+} (2.8 μ_B), that the apparent moment measured from the nearly linear part of the susceptibility at high temperature will be higher than the expected value for an isolated V^{3+} ion because of the dimer contribution. An exact calculation requires an accounting of the detailed distribution of V_n chain lengths which in turn requires a detailed model for the vanadium site disorder. It may well be that the vanadium site disorder simply represents the random introduction of additional vanadium atom vacancies into an ordered chain of dimers and vacancies of the type found in $Fe_4(PO_4)(OH)_3$ and that longer chains are not present. The good agreement between the observed data and a dimer-isolated V^{3+} model would then be expected.

The presence of additional water molecules in the structure requires comment. The number of extra water molecules observed (0.33) corresponds approximately to half the number of vanadium vacancies. Thermogravimetric analysis does not distinguish these water molecules from those associated with the framework oxygen site O2, and they are not apparent in Fourier difference maps at the end of the refinement. The extra water molecules are apparently disordered and most likely located at vacant sites in the vanadium chain and hydrogen bonded to –POH groups that are not coordinated to vanadium atoms.

On dehydration, the structural framework of $V_{1.23}(PO_4)(OH)_{0.69}(H_2O)_{0.31} \cdot 0.33H_2O$ appears to be preserved up to 750 °C. If the dehydration had occurred in a manner similar to $VO(HPO_4) \cdot 0.5H_2O$, that is, condensation of two phosphate groups to give one pyrophosphate, vanadium(III) pyrophosphate, $V_4(P_2O_7)_3$, would have been isolated;[22] however, no indications of its formation were observed. The water loss on dehydration could also be compensated structurally by transformation of the face-sharing chains into edge-sharing ones. Such a transformation could explain the structural similarities observed in the powder X-ray diffraction data of the hydrated and dehydrated phases. Without any further rearrangement, loss of water molecules from the structure would result in a lower coordination number for the vanadium(III) cations. Because vanadium(III) cations are usually only observed in octahedral coordination, a structural distortion, perhaps similar to the one observed for $MnAsO_4$, is required.[23] In $MnAsO_4$, the edge-sharing Mn(III)–oxygen octahedra are connected to form chains in a manner similar to $V_{1.23}(PO_4)(OH)_{0.69}(H_2O)_{0.31} \cdot 0.33H_2O$, except that the arsenate groups now bridge two octahedra within a chain, as well as connect

(16) Haymon, R.; Kastner, M. *Am. Mineral.* **1986**, *71*, 819.
(17) Katz, L.; Lipscomb, W. N. *Acta Crystallogr.* **1951**, *4*, 345. (b) Vencato, I.; Mattievich, E.; Mascarenhas, Y. P. *Am. Mineral.* **1989**, *74*, 456.
(18) Gorgunova, Y. E.; Linde, S. A. *Dokl. Akad. Nauk SSSR* **1979**, *245*, 584.
(19) (a) Torardi, C. C.; Calabrese, J. C. *Inorg. Chem.* **1984**, *23*, 1308. (b) Johnson, J. W.; Johnston, D. C.; Jacobson, A. J.; Brody, J. F. *J. Am. Chem. Soc.* **1984**, *106*, 8123.
(20) Torardi, C. C.; Reiff, W. M.; Takacs, L. *J. Solid State Chem.* **1989**, *82*, 203.
(21) Carlin, R. L. *Magnetochemistry*; Springer-Verlag: Berlin, 1986; p 90.
(22) Palkina, K. K.; Maksimova, S. I.; Chibiskova, N. T.; Schlesinger, K.; Ladwig, G. *Z. Anorg. Allg. Chem.* **1985**, *529*, 89.
(23) Aranda, M. A. G.; Attfield, J. P.; Bruque, S. *Inorg. Chem.* **1993**, *32*, 1925.
(24) Yvon, K.; Jeitschko, W.; Parthe, E. *J. Appl. Crystallogr.* **1977**, *10*, 73.

them to the next layer. For the dehydrated form of $V_{1.23}(PO_4)(OH)_{0.69}(H_2O)_{0.31}\cdot 0.33H_2O$ to have a similar structure, all that is required is a rotation of a phosphate group to bridge the two octahedra. The edge-sharing chain that results from the dehydration must tilt, as observed in $MnAsO_4$. No structure refinement of the X-ray data for the dehydrated form of $V_{1.23}(PO_4)(OH)_{0.69}(H_2O)_{0.31}\cdot 0.33H_2O$ was attempted because of the substantial line broadening. The data could, however, be indexed on an orthorhombic supercell with closely related lattice parameters. The relationship between the unit cells strongly suggests a close relationship between the structures of the hydrated and dehydrated compounds. The structures of the dehydrated phase and $MnAsO_4$ may also be similar though the latter has lower symmetry because of the Jahn Teller distortion of the Mn^{3+} coordination environment.

As noted above, $VPO_4\cdot H_2O$ and tetragonal phase both dehydrate to the same product. Both compounds appear to go through the same intermediate $MnAsO_4$-type phase before transforming to the high-temperature form of VPO_4. Similar behavior was also observed for $MnAsO_4\cdot xH_2O$,[23] a compound structurally related to $VPO_4\cdot H_2O$. The transformation, between the corner-sharing network and the edge-sharing network, occurs by loss of the water of hydration, and rotation of an arsenate group. A similar transformation applied to the $VPO_4\cdot H_2O$ structure results in the intermediate $MnAsO_4$-type structure, or an edge-sharing tetragonal form of VPO_4.

Conclusions

Two new hydrated vanadium(III) phosphates have been synthesized and studied by X-ray diffraction. One vanadium phosphate, $VPO_4\cdot H_2O$, is constructed of corner-sharing $[VO_6]$ octahedra and the second phase, $V_{1.23}(PO_4)(OH)_{0.69}(H_2O)_{0.31}\cdot 0.33H_2O$, is built up from face-sharing octahedra. Upon dehydration, both compounds form a tetragonal phase closely related to $MnAsO_4$, in which the vanadium/oxygen octahedra share edges.

Acknowledgment. The authors thank Dr. Kent Ross for EDX measurements and Prof. David Hoffman of the University of Houston for helpful discussions. We also thank the NSF for funding (Grant DMR-9214804) and the Robert A. Welch Foundation.